An application of laser–plasma acceleration: towards a free-electron laser amplification

OPEN ACCESS
IOP Publishing
Plasma Physics and Controlled Fusion
Plasma Phys. Control. Fusion **58** (2016) 034020 (11pp)
doi:10.1088/0741-3335/58/3/034020

An application of laser–plasma acceleration: towards a free-electron laser amplification

M E Couprie[1], M Labat[1], C Evain[2], F Marteau[1], F Briquez[1], M Khojoyan[1], C Benabderrahmane[3], L Chapuis[1], N Hubert[1], C Bourassin-Bouchet[1], M El Ajjouri[1], F Bouvet[1], Y Dietrich[1], M Valléau[1], G Sharma[1], W Yang[1], O Marcouillé[1], J Vétéran[1], P Berteaud[1], T El Ajjouri[1], L Cassinari[1], C Thaury[4], G Lambert[4], I Andriyash[4], V Malka[4], X Davoine[5], M A Tordeux[1], C Miron[1], D Zerbib[1], K Tavakoli[1], J L Marlats[1], M Tilmont[1], P Rommeluère[1], J P Duval[1], M H N'Guyen[1], A Rouqier[1], M Vanderbergue[1], C Herbeaux[1], M Sebdouai[1], A Lestrade[1], N Leclercq[1], D Dennetière[1], M Thomasset[1], F Polack[1], S Bielawski[2], C Szwaj[2] and A Loulergue[1]

[1] Synchrotron SOLEIL, l'Orme des Merisiers, Gif-sur-Yvette, France
[2] PhLAM, CERLA, Lille, France
[3] ESRF, Grenoble, France
[4] LOA ENSTA-Paristech Palaiseau, France
[5] CEA-DAM, Bruyère-Le-Châtel, France

E-mail: marie-emmanuelle.couprie@synchrotron-soleil.fr

Received 27 August 2015, revised 20 November 2015
Accepted for publication 21 December 2015
Published 17 February 2016

Abstract

The laser–plasma accelerator (LPA) presently provides electron beams with a typical current of a few kA, a bunch length of a few fs, energy in the few hundred MeV to several GeV range, a divergence of typically 1 mrad, an energy spread of the order of 1%, and a normalized emittance of the order of π.mm.mrad. One of the first applications could be to use these beams for the production of radiation: undulator emission has been observed but the rather large energy spread (1%) and divergence (1 mrad) prevent straightforward free-electron laser (FEL) amplification. An adequate beam manipulation through the transport to the undulator is then required. The key concept proposed here relies on an innovative electron beam longitudinal and transverse manipulation in the transport towards an undulator: a 'demixing' chicane sorts the electrons according to their energy and reduces the spread from 1% to one slice of a few ‰ and the effective transverse size is maintained constant along the undulator (supermatching) by a proper synchronization of the electron beam focusing with the progress of the optical wave. A test experiment for the demonstration of FEL amplification with an LPA is under preparation. Electron beam transport follows different steps with strong focusing with permanent magnet quadrupoles of variable strength, a demixing chicane with conventional dipoles, and a second set of quadrupoles for further focusing in the undulator. The FEL simulations and the progress of the preparation of the experiment are presented.

Keywords: free-electron laser, laser–plasma accelerator, undulator

(Some figures may appear in colour only in the online journal)

Introduction

Accelerator-based light sources are widely developed nowadays [1, 2]. The use of synchrotron radiation first started parasitically on high-energy physics accelerators to dedicated storage rings, and then moved onto the second generation with a few insertion devices, and onto the third generation with a high number of undulators and wigglers, with a low value of emittance, enabling partial transverse coherence, with the prospect of diffraction-limited storage rings [3]. Relativistic electrons passing through an undulator creating a periodic permanent field (period λ_u and peak magnetic field B_u in the planar case) [5] wiggle and emit radiation on a series of harmonics with the so-called resonance condition for the n-th of order harmonics $\lambda = \lambda_u(1 + K_u^2/2)/2n\Upsilon^2$, with the deflection parameter $K_u = 0.94\lambda_u(\mathrm{cm})B_u(\mathrm{T})$, and Υ the normalized electron beam energy to its rest energy. Radiation from the different periods positively interferes. Longitudinal coherence and short pulses are provided with the free-electron laser (FEL) process [6], on the so-called fourth generation light sources, leading to an increase in the peak brilliance by several orders of magnitude with respect to synchrotron radiation-based light sources. In an FEL, electrons in the undulator provide the gain medium: a light wave of wavelength λ (undulator synchrotron radiation, external seed tuned to the undulator resonant wavelength) interacts with the electron bunch, inducing an energy modulation of the electrons, which is gradually transformed into density modulation at λ, enabling phased electrons to coherently emit emission at λ and its harmonics of order n. The light wave-electron interaction can lead to a light amplification to the detriment of the kinetic energy of the electrons. The small signal gain is proportional to the electronic density and varies as the inverse of the cube of the electron beam energy, depending on the undulator length. The FEL wavelength is tuned by changing the undulator magnetic field in a given spectral range set by the electron beam energy. The polarization depends on the undulator configuration.

FEL radiation was first observed in infra-red, using a linear accelerator [7, 8], then on a storage ring in the visible [9], UV [10–12] and in the VUV [13–15] thanks to the coherent harmonic generation process [16]. Meanwhile, FEL oscillators were built whereas the high gain theory was developed [17–19] and the self-amplified spontaneous emission (SASE) concept was proposed [20–24]. Nowadays, more than fifty years after the laser discovery [25], x-ray FEL user facilities offer high brilliance femtosecond tunable radiation in the x-ray domain with the hard x-ray range covered by LCLS [26] and SACLA [27], and the soft x-ray by FLASH [28] and FERMI [29]. FEL oscillators being limited to VUV [30, 31], single-optical-pass FEL devices are preferred for short wavelength operation, either in the SASE configuration, self-seeded [32–35] or in the external seeding one [36–39] such as FERMI, enabling one to reduce the intrinsic SASE spikes, jitter and intensity fluctuations and to improve the spectral purity.

Besides the preparation of additional FEL light sources, the evolution trend of FEL development is twofold. First, it aims at implementing advanced seeding schemes [40–49] for somehow controlling the FEL longitudinal properties, at providing improved FEL performance (such as two-color operation [50–58], ultra-short pulses (see for example [59–66]) or narrow bandwidth [67], high peak power, high repetition rate, and multi-user operation [68]. Second, in the quest for compactness one must consider replacing one of the components by an alternative: it can be the case for the undulator [69] or for the linear accelerator by using systems from new emerging concepts such as laser plasma acceleration [70, 71], dielectric acceleration [72], and inverse FEL [73, 74]. Here, we report the upcoming FEL amplification studies with a laser plasma accelerator (LPA), which will be performed according to a COXINEL (coherent x-ray source inferred from electrons accelerated by laser) test program, in the context of the LUNEX5 demonstrator of an advanced and compact FEL [75, 76, 77] (see figure 1). Adopted strategies to answer the requirements for FEL in terms of beam manipulation are discussed. The test experiment under preparation with various hardware components is described.

1. Strategies for LWFA beam handling for FEL application

In a laser–plasma wakefield accelerator [78–80], an intense laser pulse is focused in a light gas or in a mixture of heavy and light gases [81]. The rising edge of the laser ionizes the gas and creates a plasma. As the laser pulse propagates in the plasma, the ponderomotive force expels electrons from the optical axis, thus forming a cavity free of electrons in the laser wake. The fields in this cavity have very large amplitudes, up to hundreds of gigaelectronvolts by meters. As a result, electrons trapped in the cavity can be accelerated to gigaelectronvolt energies in just a few millimeters.

For now, the stable and controlled injection of electrons into the accelerating plasma cavities remains an important challenge, and considerable effort has been made for many years to establish such a control, and thus to improve the quality of the resulting beams. For this, a wide range of injection techniques was considered theoretically and experimentally, e.g. injection-colliding laser pulses [82], density transition injection [83], near-threshold injection [84], ionization injection [85], etc. Typical electron beams have energies of a few hundred MeV (up to 4 GeV [86, 87]), charges of a few tens of picocoulomb, femtosecond durations [88], relative energy spreads of a few percent (1% at best [89]) and emittances below 1 μm [90]. Electron beam performance [91–95] depends on the

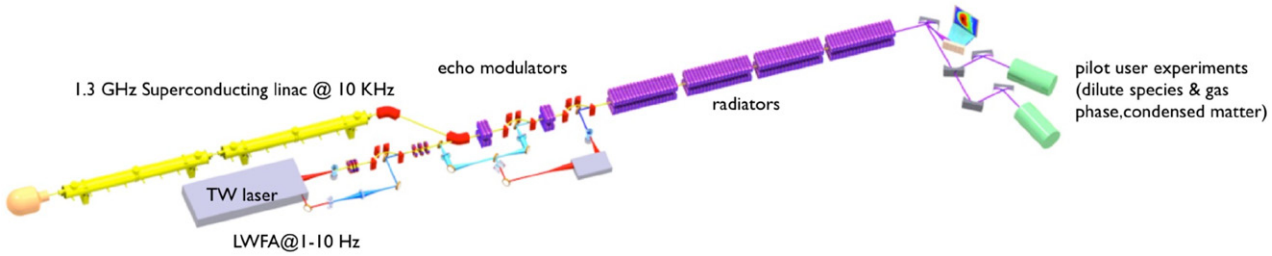

Figure 1. Sketch of the LUNEX5 (free-electron laser using a new accelerator for the exploitation of x-ray radiation of 5th generation) demonstrator of advanced and compact FEL in the 4–40 nm spectral range with 20 fs FEL pulses. LUNEX5 comprises two accelerators: a superconducting one for high repletion rate operation and multi-user operation, and a laser plasma accelerator to be qualified by the FEL application. The single FEL line will be composed of the most advanced seeding configurations: seeding with HHG (high order harmonics generated in gas), EEHG (echo-enable harmonic generation) and will be terminated by pilot-user experiments to characterize and evaluate the performance of these sources from a user perspective.

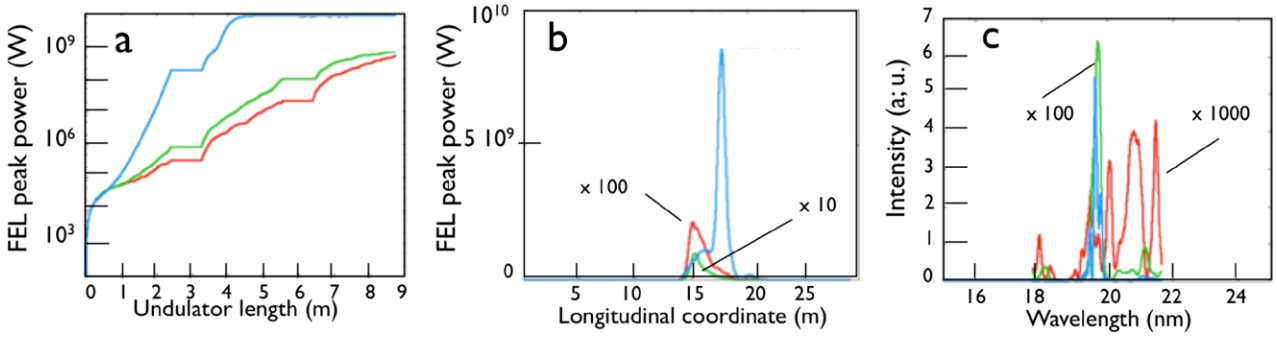

Figure 2. FEL performance at 19.5 nm in the SASE configuration with an LWFA beam: (a) FEL peak power versus undulator length, (b) Longitudinal profile of FEL pulse, (c) Spectral profile of FEL pulse. Electron bunch: $E = 400$ MeV, energy spread of 0.1% (blue), 0.5% (green) and 1% (red), peak current of 10 kA, electron bunch duration of 2 fs rms, emittance = 1.0 π.mm.mrad. Undulator: 200 periods of 12 mm, $K = 1.408$.

adopted configuration, and typically one can consider getting a few hundred MeV electron beam of tens of pC charge, with 1 μm transverse size, 1 mrad divergence with 1 μm longitudinal size (normalized emittance of 1 π.mm.mrad), few femtosecond duration and 1% energy spread, i.e. two orders of magnitude larger energy spread and three orders of magnitude larger divergence than electrons issued from a conventional linear accelerator, while the electron bunch is generally rather short. Without appropriate electron beam transport, the electron bunch length and emittance cannot be preserved, because of the large electron beam divergence [96–98]. The beam divergence requires a strong focusing with adapted quadrupoles of high gradient close to the electron source and/or with a plasma lens [97]. So far, only LWFA-based undulator spontaneous emission has been observed [99–103].

However, in view of an FEL application [104–108], the large energy spread value is also an issue. Two strategies of longitudinal beam manipulation are considered. The first consists of passing the electron beam through a decompression chicane, which sorts the electrons according to their energy and can typically reduce the slice energy spread, a critical feature for the FEL application, by one order of magnitude [109–111]. Moreover, taking advantage of the introduced correlation between the energy and the position, the slices can be focused in synchronization with the optical wave advance, in the so-called chromatic matching scheme [112], resulting in an additional spatial manipulation. Test experiments are under preparation at Berkeley [113, 114], CFEL [115], and SOLEIL in collaboration with Laboratoire d'Optique Appliquée and Univ. Lille [116–118]. The second concept for handling the large energy spread of LWFA consists of using a transverse gradient undulator [119–121] creating an additional transverse focus thanks to canted magnetic poles in addition to the longitudinal periodic magnetic field. A linear transverse dependence of the vertical undulator field is thus generated, according to $K(x) = K_0(1 + \alpha x)$ with α the gradient coefficient. Associated to optics with dispersion introducing a transverse displacement x with the energy according to $x = \eta\Delta\gamma/\gamma$, the resonant condition is fulfilled for $\eta = (2 + K_o^2)/\alpha K_o^2$ even though the initial energy spread is larger. Consequences for the FEL features have been further investigated [122–124]. An experimental implementation of such a scheme is under progress at F. Shiller Univ., Jena, in collaboration with KIT [125, 126] with a superconducting transverse gradient undulator (TGU) [127–130].

2. Towards LWFA FEL amplification: beam manipulation on COXINEL

First, assuming that the electron beam is directly transported and focused in the undulator in the case of LUNEX5, one can examine what could be done in terms of the FEL with the LPA. Figure 2 illustrates GENESIS [131] calculations performed

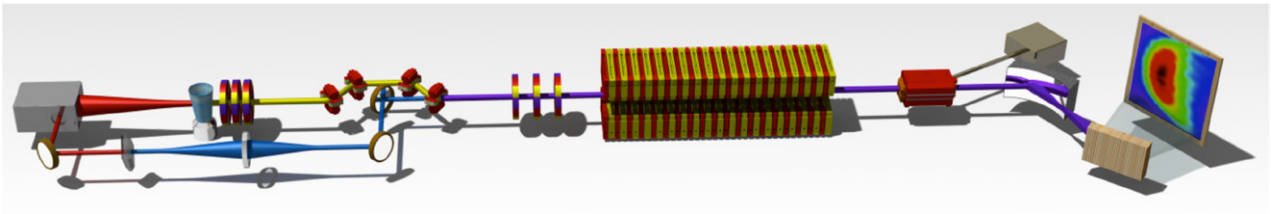

Figure 3. Sketch of the proposed beam transfer line from the laser hutch and electron beam generation in the gas cell, including the seed and down to the FEL diagnostic station.

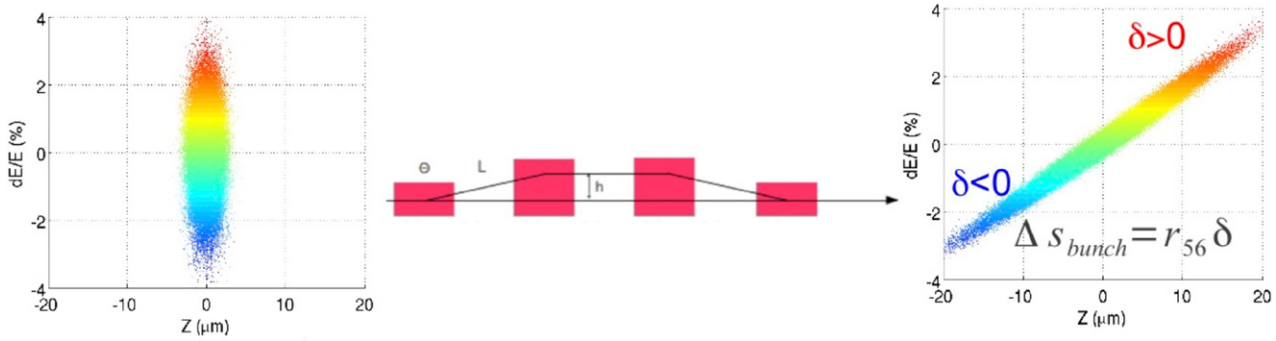

Figure 4. Effect of the chicane on the electron beam longitudinal properties. Longitudinal phase space before (left) and after (right) the chicane. d*E*/*E*: relative energy difference, *Z*: longitudinal position.

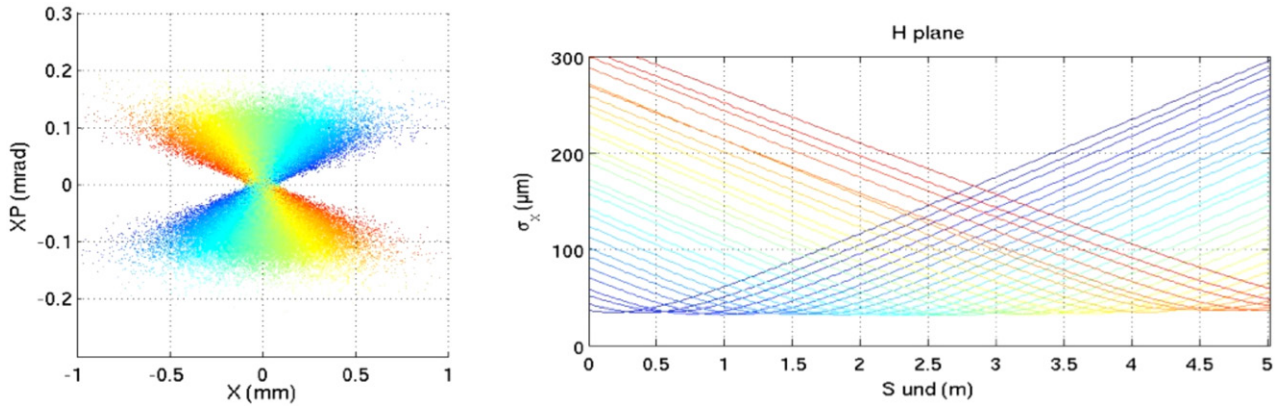

Figure 5. Schematic of the chromatic matching: left transverse phase (X: horizontal position, XP: horizontal angle): right: transverse size along the longitudinal position along the undulator.

at 19.5 nm for different values of the energy spread 0.1, 0.5 and 1%. Figure 2(a) shows the FEL amplification while the electron bunch is progressing inside the undulator segments (between the segments, amplification is stopped and the signal remains constant). Only in the case of 0.1% energy spread, does the FEL power reach the usual GW peak power level. Figure 2(b) exhibits the longitudinal distribution of the radiation. The shape of the pulse is deformed in the 0.5 and 1% energy spread case, the longitudinal coherence is not properly built and the FEL is not yet properly established. Figure 2(c) shows the spectral profile of the radiation in the three cases of energy spread: it is extremely noisy in the 1% energy spread case and does not have the expected laser properties. Only the case of an energy spread of 0.1% exhibits nice spectral and temporal profiles. It is also highly optimistic since the electron beam parameters have been directly introduced in the FEL simulations without taking into account the electron beam degradation that might occur during its transport to the undulator. Another more secure solution has thus to be implemented.

In order to have a more reasonable approach, a dedicated transfer line enabling manipulation of the electron beam properties has been designed, as shown in figure 3. The experiment is first set for a 200 nm operation with a 180 MeV electron beam, before going at a shorter wavelength (aiming at 40 nm) with a 400 MeV electron beam. The optimization at 180 MeV is described here.

The intense laser is focused down to a gas cell for the electron production. The electron beam transport line is composed of a first triplet of quadrupoles located just after the gas cell, a chicane of four dipoles for the decompression (see figure 3) and a seeding port. Figure 3 shows the effect of the chicane on the longitudinal phase space. The electrons are sorted according to their energy, the slice energy spread is reduced, and the electron bunch is lengthened.

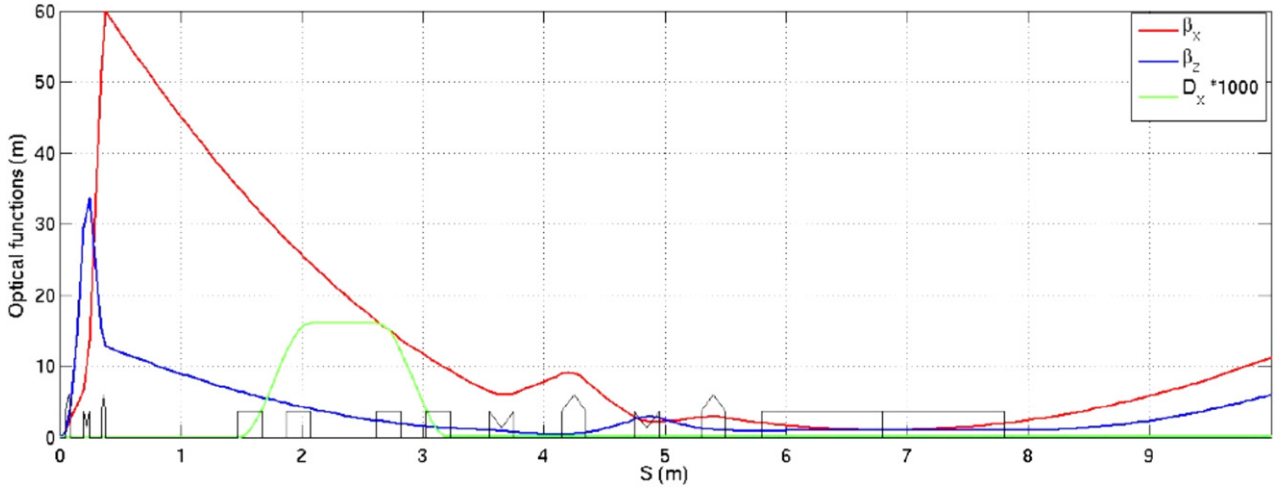

Figure 6. Optical functions along the COXINEL line at 180 MeV.

Then, the transport line accommodates a second set of quadrupoles for performing the adequate focusing for proper interaction between the electrons and photons, the undulator, an electron beam dump, and a monochromator. The chromatic matching can be applied, as shown in figure 5. Four correctors are also set along the transport, two surrounding the chicane and two the undulator.

Electron linear optics have been designed [132] to image the source in the undulator, with a magnification of 20, and to synchronize the electron bunch slice focus, together with the optical wave propagation according to the chromatic matching concept [112] using BETA [133] code associated to a 6D sympletic tracking and ASTRA [134]. A Gaussian distribution has been considered for the transport and FEL optimization, intending first to cope with the large values of the energy spread and divergence. These types of distributions provide a first basis for the understanding and optimization of the electron beam dynamics. In reality, LPA beams have a more complicated phase structure, such as energy chirp [135] but the concept of chromatic matching should also be suitable in principle to handle the chirp in the LPA electron beams. Indeed, a linear chirp would only induce a small shift in the chicane strength, which is a scanned parameter.

The optical functions are shown in figure 6. The maximum electron beam deviation in the chicane is 32 mm.

The nonlinear study considers, in addition, the contribution of the chromatic emittance, and the additional sources of bunch lengthening. The natural undulator focusing is also taken into account. Collective effects such as space charge and coherent synchrotron radiation have also been considered. They lead to a slight increase in the emittance, with respect to the case neglecting these collective effects. Impedance and resistive wall have still to be included. The main obtained COXINEL parameters for the 180 MeV case are listed in table 1. The dipoles enable an 80 mrad deviation and give a maximum bunch decompression strength $r_{56} = 4.3$ mm at 400 MeV.

Two different undulators will be used. Their characteristics are given in table 2. The seeded FEL power calculated with the baseline parameters for the 200 and 40 nm cases versus the chicane strength is plotted in figure 7. The optimum is rather smooth and differs in the two operating points. The FEL power is amplified by several orders of magnitude and it reaches the 10 MW range. The FEL pulse duration is typically 15 fs FWHM. The FEL performance is, however, highly dependent on the electron beam characteristics. Getting the FEL amplification is still very challenging.

Table 1. Main COXINEL electron parameters at 180 MeV.

Electron characteristics		Cell exit	Undulator entrance
Energy	MeV	180	180
Normalized emittance total	π.mm.mrad	1	2.4
Normalized emittance slice		1	1.3
Divergence	mrad	1	20
Size	μm	1	60 (slice)
Duration	fs	3.3	36
Charge	pC	34	
Peak current	kA	4	0.5
Energy spread total	%	1	1.1
Energy spread slice	%	1	0.13

3. Towards LWFA FEL amplification: experiment preparation on COXINEL

3.1. General integration

Even though the acceleration process in plasma is very compact, the necessary electron beam manipulation requires some magnetic elements, diagnostics and the overall implementation is not straightforward. In the COXINEL planned experiment, the transfer line equipment is designed, built and measured at SOLEIL before being implemented in the Salle Jaune of Laboratoire d'Optique Appliquée, where the electrons are generated. The general integration had to fit in 11 m from the electron source to the end of the FEL characterization equipment (see figure 8). In order to accommodate the different components in the available space, steerers, one cavity beam position monitor and diagnostics have been set just after the permanent magnet quadrupoles. The first triplet of quadrupoles, one current

Table 2. COXINEL undulator characteristics.

Characteristics	Unit	U20	U15
Period	mm	20	15
Number of periods		98	200
Minimum gap	mm	5.5	3
Peak field (293 K)	T	1	1.53
Peak field (77 K)	T	1.53	1.65
Technology		In-vacuum, hybrid	Cryo-ready, hybrid
Permanent magnets		Nd2Fe14B	Pr2Fe14B
Poles		Vanadium Permendur	Vanadium Permendur

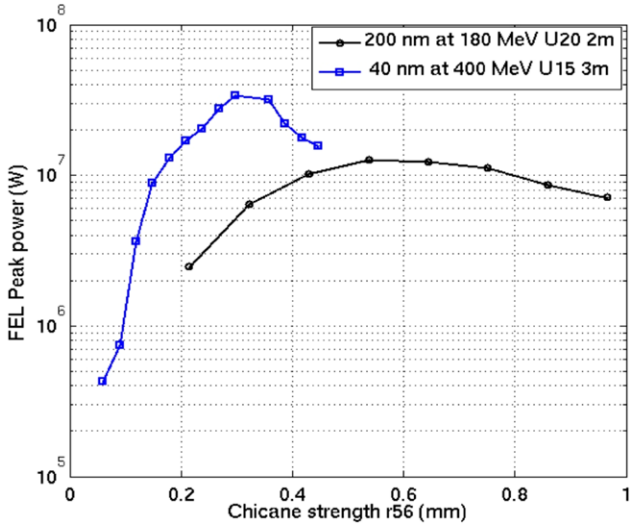

Figure 7. FEL power for the 200 nm case and for the 40 nm case versus the chicane strength. Parameters of tables 1 and 2, seed of 10 kW.

transformer and the first steerer will also be put directly into the chamber containing the gas cell.

The vacuum level will be about 10^{-4} mbar in the gas jet area. In the transfer line, three turbo-molecular pumps, connected by soft bellows for limiting the vibration level are implemented all along the line, enabling them to reach a 10^{-6} mbar level. The usual ionic pumps of the undulator are changed to turbo-molecular ones.

3.2. Laser–plasma acceleration of electrons

Electrons will be generated with the Salle Jaune laser facility at LOA which delivers two 60 TW laser pulses at a central wavelength of 810 nm. The energy in each beam is about 1.6 J and the laser duration is 28 fs. One of the beams will be focused in a supersonic helium gas jet or in a gas mixture, with an *f*/15 off-axis parabola mirror. A controlled injection technique, such as colliding injection [82] or density transition injection [85] will be used to produce a stable electron beam with energy of 180 MeV, a divergence below 2 mrad and a relative energy spread below 3%. A laser–plasma lens [99] could be used to reduce the beam divergence below 1 mrad.

A leak of the main Ti–Sa laser driving the electron generation will also be used to generate high-order harmonics in gas, to be used as a seed. The seeding light will be injected via a viewport using a mirror located in the middle of the chicane. Different mirror systems will be chosen for the different spectral ranges.

Table 3. Magnetic elements of the COXINEL transport line.

Component	Characteristics	Unit	Value
First triplet of quadrupoles	Gradient (180 MeV)	T m^{-1}	102/− 103/91
	Gradient (400 MeV)	T m^{-1}	142.2/142.3/133.4
	Bore diameter	mm	12
Chicane	Dipole field	T	0.565
	Gap	mm	25
	Maximum deviation	mT m	132
Dipole power supply	Current	A	150
	Voltage	V	8
	Accuracy	ppm	15
Second set of quadrupoles	Gradient	T m^{-1}	20
	Bore diameter	mm	25
	Length	mm	200
Steerers	Field	T	0.35
Steerer/quadrupole power supplies	Current	A	10
	Voltage	V	10
	Accuracy	ppm	20
Beam dump dipole	Field	T	1

3.3. Magnetic elements and power supplies of the transport line

The characteristics of the COXINEL magnetic elements are listed in table 3. The magnetic elements have been designed and optimized with respect to the electron beam dynamics using RADIA [136] and TOSCA [137] magnetic software.

The first triplet is made of permanent magnet quadrupoles (so-called QUAPEVA) enabling it to achieve the required strength for the given bore diameter. A specific design has been carried out in TOSCA to enable sufficient strength variation. It is under preparation in collaboration with Sigmaphi.

The chicane is composed of four identical water-cooled electromagnetic dipoles. Manufactured by SEF, they have been measured at SOLEIL with a rotating coil and a Hall probe. The measured field integrals, as shown in figure 9(a), are in agreement with the expected calculations from the RADIA and TOSCA models. A magnetic-field mapping is presented in figure 9(b). A good agreement is obtained between

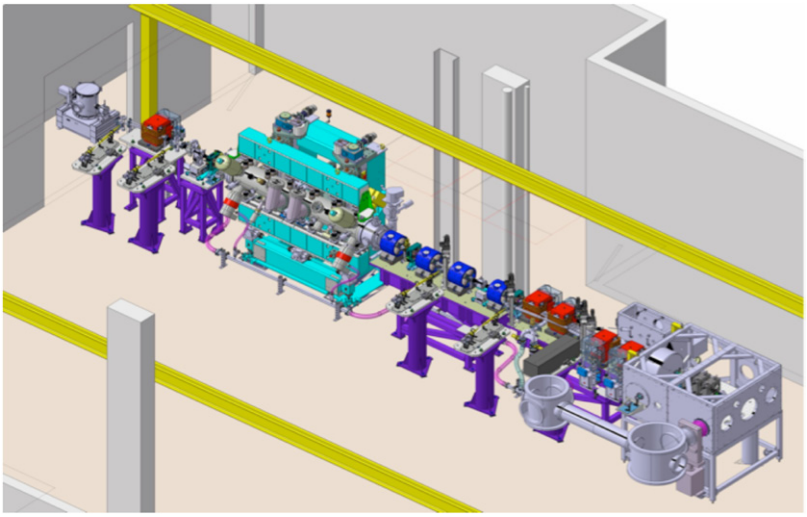

Figure 8. CATIA general integration of the COXINEL experiment (in red, the dipole chicane, in blue, the quadrupoles, in light blue, the undulator, in green, the steerers).

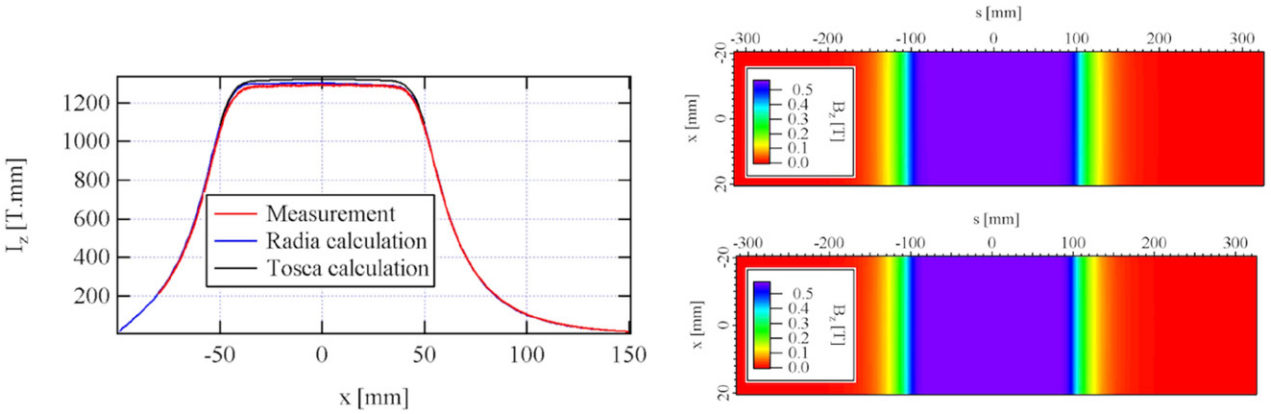

Figure 9. Measurement of a COXINEL dipole (a) field integral measurement with a rotating coil versus the transverse direction compared to the RADIA and TOSCA models, (b) field-mapping measurement along the longitudinal co-ordinate with a Hall probe compared to the field-map calculation with RADIA.

simulations and measurements. Four independent bipolar power supplies feed the dipoles. The power supplies (manufactured by Sigmaphi Electronics) are tested at SOLEIL.

The quadrupoles of the second set are electromagnetic air-cooled components. They are manufactured by SEF. The steerers are air-cooled electromagnetic devices, also manufactured by SEF.

The steerer and quadrupole power supplies ($\pm$10 A, 10 V, 16 bit resolution) are bipolar. They are manufactured by Sigmaphi Electronics.

The beam dump dipole is constituted of permanent magnets.

3.4. Diagnostics

3.4.1. Electron diagnostics. The interceptive position and transverse measurements of the electrons by imaging the electron beam hitting one screen inserted at 45°, are established thanks to the diagnostic stations [138]. These stations include a translation stage with an OTR screen, a YAG:Ce or LYSO:Ce screen and calibration grid, associated with a re-imaging achromatic system on a CCD camera (Basler series scA640-70gm) with two magnifications enabling one to adjust the resolution depending on the purpose. A set of neutral densities is mounted on a motorized filter wheel to adapt the incident intensity on the CCD. Since coherent optical transition radiation can become an issue, appropriate simulations are in progress. There are six of them, installed at different locations (just after the first triplet, in the chicane, on the first beam dump, at the entrance and exit of the undulator, and on the final beam dump).

Non-interceptive beam position measurements will be done with two cavity beam position monitors (cavity BPM) from the Paul Sherrer Institute [139], to be installed at the entrance and exit of the undulator. The expected resolution is below 1 μm even at low charge. In addition, a stripline, under design at SOLEIL, will provide a resolution of 30 μm at 1 pC. It will be easier to operate. It will be installed at the exit of the undulator.

The electron beam energy and energy spread can be measured using a standard imager after a dipole magnet in a dispersive section of the transport beam line.

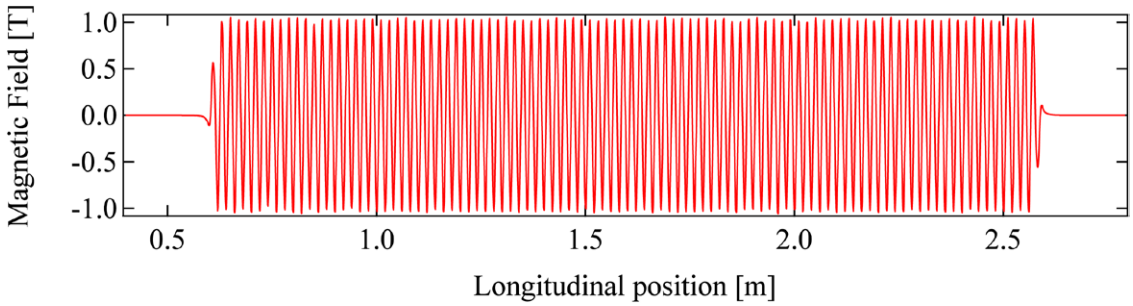

Figure 10. Magnetic measurement of the U20 undulator to be used for the COXINEL.

The electron beam charge will be measured just after the first triplet and at the undulator exit, using a commercial integrated current transformer (ICT) (Bergoz) adapted from a low charge (10 pC).

The ICT and the cavity BPM are under test on the Synchrotron SOLEIL transfer line. So far, expected performances are currently being achieved.

3.4.2. Photon diagnostics. The spectral measurement (spontaneous emission, seed, FEL) will be done using a spectrometer located 3 m downstream from the undulator exit. First, for the UV-visible spectral range, an iHR320 spectrometer (Horiba), equipped with a Synapse back-illuminated CCD and a plane holographic grating, will enable single-shot measurement of the radiation spectrum. For a shorter wavelength, the use of a customized version of a PGM200 spectrometer (Horiba) is foreseen and under investigation. By coupling a toroidal mirror and a set of planar gratings, this device will enable the measurement of spectra from 200 down to 10 nm.

3.5. Undulators

The first 2 m long in-vacuum hybrid undulator is already built. The magnetic field measurement is shown in figure 10. Then, a 3 m long U15 cryo-ready undulator will be employed. Following the cryogenic undulator built with $Pr_2Fe_{14}B$ magnets first developed at SOLEIL [140, 141], a typical LUNEX5 U15 module is developed by a French–Swedish collaboration. The use of a $Pr_2Fe_{14}B$ specific grade with poles in VanadiumPermendur enables operation both at room temperature and at 77 K. The module scheme has been modified for using half-poles, enabling an easier swapping [142, 143].

4. Conclusion and prospects

Recently, tremendous progress has been achieved on electron beam accelerated by laser– plasma interaction. Even though these beams cannot compete yet with electron beam produced by conventional accelerators in terms of energy spread and divergence, it is worth discussing their applications. As an intermediate, before considering future linear colliders based on LPA, it appears that an FEL application could qualify LPA beams, even though achieving an FEL amplification with electrons produced by laser–plasma acceleration is very challenging. Considering electron beam parameters at the limit of what has been measured so far, the simulations presented here show that amplification is possible, providing an adapted transfer line for the manipulation of the electron beam properties in view of the FEL. This manipulation enables one to handle both the electron beam divergence with a first strong focusing, and then to cope with the large energy spread in sorting out the electrons, thus reducing the slice energy spread. In addition, the concept of chromatic matching presented here enables one to turn into advantage the energy to transverse phase-space correlation inside the bunch, for an adapted focusing inside the undulator. Prior to experimental tests to be performed according to the COXINEL studies, such a design requires the optimization and preparation of a significant amount of hardware for the transfer line to the undulator, necessary for enabling the FEL amplification. Issues related to the electron beam stability and repeatability will be even more of a challenge to get the amplification signal.

Acknowledgments

This work was supported by the European Research Council under Grant COXINEL (number 340015); X-FIVE (339128), the Triangle de la Physique for the QUAPEVA valorization contract, the Laboratoire d'Excellence Physique Atomes Lumière Matière- ANR-10-LABEX-0039 (FEL shaping). M E Couprie, C Benabderrahmane and F Briquez acknowledge the French–Swedish collaboration for the support on the U15 cryo-ready undulator. C Benabderrhamane, M E Couprie and F Marteau are thankful for the support from the 'Triangle de la Physique' for the QUAPEVA valorization contract and to J L Lancelot, F Forest and O Cosson from Sigmaphi for their involvement in the project.

References

[1] Couprie M E and Filhol J M 2008 X radiation sources based on accelerators *C.R. Phys.* **9** 487–506
[2] Couprie M E 2014 *J. Electron Spectrosc. Relat. Phenom.* **196** 3–13
[3] Couprie M E and Valléau M 2012 Radiation, polarisation, devices, new sources, VIth International School on 'Magnetism and Synchrotron Radiation: Towards the Fourth Generation Light Sources' *Proc. of the 6th Int. School 'Synchrotron Radiation and Magnetism' (Mittelwihr, France)* Series: Springer

Beaurepaire E, Bulou H, Joly L and Scheurer F (ed) 2013 *Proc. in Physics* vol 151 XVIII (344 pages), pp 51–94, over 344 pages
[4] Borland M 2012 Progress towards ultimate storage ring light sources *Proc. of IPAC 2012 (New Orleans, Louisiana, USA)* pp 1035–9
[5] Madey J M J 1971 Stimulated emission of Bremmstrahlung in a periodic magnetic field *Appl. Phys.* **42** 1906
[6] Elias L *et al* 1976 Observation of the stimulated emission of radiation by relativistic electrons in a spatially periodic transverse magnetic field *Phys. Rev. Lett.* **36** 717–20
[7] Deacon D A G *et al* 1977 *Phys. Rev. Lett.* **38** 892–4
[8] Billardon M, Elleaume P, Ortega J M, Bazin C, Bergher M, Velghe M, Petroff Y, Deacon D A G, Robinson K E and Mady J M J 1983 First operation of a storage-ring free-electron laser *Phys. Rev. Lett.* **51** 1652
[9] Kulipanov G N *et al* 1990 *Nucl. Instrum. Methods* A **296** 1
[10] Couprie M E, Garzella D, Delboulbé A, Velghe M and Billardon M 1993 Operation of the Super-ACO FEL in the UV range at 800 MeV *Europhys. Lett.* **21** 909–14
[11] Hama H, Kimura K, Yamazaki J, Takano S, Konishita T and Couprie M E 1996 Microscopic study on lasing characteristics of the UVSOR storage ring free electron laser *Nucl. Instrum. Methods* A **375** 39–45
[12] Girard B, Lapierre Y, Ortega J M, Bazin C, Billardon M, Elleaume P, Bergher M, Velghe M and Petroff Y 1984 Optical frequency multiplication by an optical klystron *Phys. Rev. Lett.* **53** 2405
[13] Prazeres R, Ortéga J M, Bazin C, Bergher M, Billardon M, Couprie M E, Fang H, Velghe M and Petroff Y 1987 First production of vacuum-ultraviolet coherent light by frequency multiplication in a relativistic electron beam *Europys. Lett.* **4** 817–22
[14] Prazeres R *et al* 1991 Coherent harmonic generation in VUV with the optical klystron on the storage ring super-ACO *Nucl. Instrum. Methods* A **304** 72–6
[15] Coisson R *et al* 1982 *Phys. Quantum Electron.* **9** 939
[16] Kroll N M and McMullin W A 1978 Stimulated emission from relativistic electrons passing through a spatially periodic transverse magnetic field *Phys. Rev.* A **35** 3406–23
[17] Dattoli G, Marino A, Renieri A and Romanelli F 1981 Progress in the Hamiltonian picture of the free-electron laser *IEEE J. Quantum Electron.* **17** 1371–87
[18] Haus H 1981 Noise in free-electron laser amplifier *IEEE J. Quantum Electron.* **17** 1427–35
[19] Kondratenko A M *et al* 1979 *Sov. Phys. Dokl.* **24** 989
[20] Kondratenko A M and Saldin E L 1980 Generation of coherent radiation by a relativistic electron beam in an undulator *Part. Acc.* **10** 207
[21] Derbenev Y S, Kondratenko A M and Saldin E L 1982 On the possibility of using a free electron laser for polarization control in a storage ring *Nucl. Instrum. Methods* A **193** 415
[22] Kim K J *et al* 1986 *Phys. Rev. Lett.* **57** 1871
[23] Bonifacio R, Pelligrini C and Narducci L M 1984 Collective instabilities and high gain regime in a free electron laser *Opt. Commun.* **50** 373–8
[24] Bonifacio R, De Salvo L, Pierini P, Piovella N and Pellegrini C 1994 *Phys. Rev. Lett.* **73** 70
[25] Schawlow A L and Townes C H 1958 Infra-red and optical masers *Phys. Rev.* **112** 1940–9
[26] Emma P *et al* 2010 First lasing and operation of an ångstrom-wavelength free-electron laser *Nat. Photon.* **4** 641
[27] Ishikawa T *et al* 2012 A compact x-ray free-electron laser emitting in the sub-ångström region *Nat. Photon.* **6** 540–4
[28] Ackermann W *et al* 2007 Operation of a free-electron laser from the extreme ultraviolet to the water window *Nat. Photon.* **1** 336–42
[29] Allaria E *et al* 2012 Highly coherent and stable pulses from the FERMI seeded free-electron laser in the extreme ultraviolet *Nat. Photon.* **6** 699–704
[30] Marsi M *et al* 2002 Operation and performance of a free electron laser oscillator down to 190 nm *Appl. Phys. Lett.* **80** 2851–3
[31] Trovò M *et al* 2002 Operation of the European storage ring FEL at ELETTRA down to 190 nm *Nucl. Instrum. Methods* A **483** 157–61
[32] Geloni G L 2011 A novel self-seeding scheme for hard x-ray FELs *J. Mod. Opt.* **58** 1391–403
[33] Amann J *et al* 2012 Demonstration of self-seeding in a hard-x-ray free-electron laser *Nat. Photon.* **6** 693–8
[34] Inagaki T *et al* 2014 Stable generation of high power self-seeded XFEL at SACLA *Proc. of IPAC 2014* pp 15–20
[35] Ratner D *et al* Experimental demonstration of a soft x-ray self-seeded free electron laser SLAC-PUB-16214
[36] Yu L H and Ben-Zvi I 1997 High-gain harmonic generation of soft x-rays with the 'fresh bunch' technique *Nucl. Instrum. Methods* A **393** 96
[37] Yu L H *et al* 2000 *Science* **289** 932
[38] Dattoli G, Ottaviani P L and Pagnutti S 2005 Nonlinear harmonic generation in high-gain free-electron lasers *J. Appl. Phys.* **97** 113102
[39] Lambert G *et al* 2008 Injection of harmonics generated in gas in a free-electron laser providing intense and coherent extreme ultraviolet light *Nat. Phys.* **4** 296–300
[40] Togashi T *et al* 2011 *Opt. Express* **1** 317–24
[41] Labat M *et al* 2011 *Phys. Rev. Lett.* **107** 224801
[42] Ackermann S *et al* 2013 *Phys. Rev. Lett.* **111** 114801
[43] Lambert G *et al* 2009 *Europhys. Lett.* **88** 54002
[44] Tanikawa T *et al* 2011 Nonlinear harmonic generation in a free-electron laser seeded with high harmonic from gas *Europhys. Lett.* **3** 34001
[45] Stupakov G 2009 *Phys. Rev. Lett.* **102** 074801
[46] Xiang D *et al* 2010 *Phys. Rev. Lett.* **105** 114801
[47] Hemsing E *et al* 2014 *Phys. Rev. Spec. Top.—Accel. Beams* **17** 070702
[48] Zhao Z T *et al* 2012 First lasing of an echo-enabled harmonic generation free-electron laser *Nat. Photon.* **6** 360–3
[49] Prazeres R, Glotin F, Insa C, Jaroszynski D A and Ortega J M 1998 Two colour operation of a free electron laser and applications in the mid-infrared *Eur. Phys. J.* **D3** 87
[50] Lutman A *et al* 2013 Experimental demonstration of fs two-color x-ray FELs *Phys. Rev. Lett.* **110** 134801
[51] Marinelli A *et al* 2013 Multicolor operation and spectral control in gain-modulated x-ray free electron laser *Phys. Rev. Lett.* **111** 134801
[52] Hara T *et al* 2013 Two-colour hard x-ray free-electron laser with wide tunability *Nat. Commun.* **4** 2919
[53] Marinelli A *et al* 2015 High-intenisty double-pulse x-ray free-electron laser *Nat. Commun.* **6** 6369
[54] Labat M, Joly N, Bielawski S, Swaj C, Bruni C and Couprie M E 2009 Pulse splitting in short wavelength free electron laser *Phys. Rev. Lett.* **103** 264801
[55] De Ninno G *et al* 2013 *Phys. Rev. Lett.* **110** 064801
[56] Allaria E *et al* 2013 *Nat. Commun.* **4** 2476
[57] Petralia A *et al* 2015 *Phys. Rev. Lett.* **115** 014801
[58] Emma P 2004 *Phys. Rev. Lett.* **92** 074801
[59] Zholents A A and Fawley W 2004 *Phys. Rev. Lett.* **92** 224801
[60] Saldin E *et al* 2004 *Opt. Commun.* **239** 161
[61] Saldin E *et al* 2006 *Phys. Rev. Spec. Top.—Accel. Beams* **9** 050702
[62] Zholents A *et al* 2008 *New J. Phys.* **10** 025005
[63] Tanaka T 2013 *Phys. Rev. Lett.* **110** 084801
[64] Dunning D J *et al* 2013 *Phys. Rev. Lett.* **110** 104801
[65] Prat E and Reich S 2015 *Phys. Rev. Lett.* **114** 244801
[66] Bourassin-Bouchet C and Couprie M E 2015 Partially coherent ultrashort spectrography *Nat. Commun.* **6** 6465

[67] Kim K J *et al* 2008 *Phys. Rev. Lett.* **100** 244802
[68] Hara T *et al* 2013 Time interleaved multienergy acceleration for a x-ray free electron facility *Phys. Rev. Spec. Top.—Accel. Beams* **16** 080701
[69] Couprie M E *et al* 2015 Cryogenic undulators *Proc. SPIE (Prague, April 2015)*
[70] Tajima T and Dawson J M 1979 Laser electron accelerator *Phys. Rev. Lett.* **43** 267
[71] Malka V *et al* 2011 Principle and applications of compact laser-plasma electron accelerator *Nat. Phys.* **7** 219
[72] Naranjo B, Valloni A, Putterman S and Rosenzweig J B 2012 Stable charge-particle acceleration and focusing in a laser accelerator using spatial harmonics *Phys. Rev. Lett.* **109** 176803
[73] Kimura W *et al* 2004 *Phys. Rev. Lett.* **92** 154801
[74] Musumeci P *et al* 2005 *Phys. Rev. Lett.* **94** 154801
[75] Couprie M E *et al* 2012 The LUNEX5 project in France *J. Phys. Conf. Ser. 2013* **425** 072001 (SRI2012)
[76] Couprie M E *et al* 2015 Strategies towards a compact XUV free electron laser adopted for the LUNEX5 project Accepted in *J. Mod. Opt.* (DOI: 10.1038/nphoton.2013.277)
[77] Couprie M E *et al* 2015 Progress of the LUNEX5 project *Proc. IPAC 2015 (Richmond, USA)*
[78] Mangles S *et al* 2004 *Nature* **431** 535
[79] Faure J *et al* 2004 *Nature* **431** 541
[80] Geddes C G R *et al* 2004 High-quality electron beams from a laser wakefield accelerator using plasma-channel guiding *Nature* **431** 538–41
[81] Chen M, Sheng Z-M, Ma Y-Y and Zhang J 2006 *J. Appl. Phys.* **99** 056109
[82] Faure J, Rechatin C, Norlin A, Lifschitz A, Glinec Y and Malka V 2006 *Nature* **444** 737
[83] Schmid K, Buck A, Sears C M S, Mikhailova J M, Tautz R, Herrmann D, Geissler M, Krausz F and Veisz L 2010 *Phys. Rev. Spec. Top.—Accel. Beams* **13** 091301
[84] Banerjee S *et al* 2013 *Phys. Rev. Spec. Top.—Accel. Beams* **16** 031302
[85] Yu L-L, Esarey E, Schroeder C B, Vay J-L, Benedetti C, Geddes C G R, Chen M and Leemans W P 2014 *Phys. Rev. Lett.* **112** 125001
[86] Wang X *et al* 2013 Quasi-monoenergetic laser-plasma acceleration of electrons to 2 GeV *Nat. Commun.* **4** 1988
[87] Leemans W P *et al* 2014 Multi-GeV electron beams from capillary-discharge-guided subpetawatt laser pulses in the self-trapping regime *Phys. Rev. Lett.* **113** 245002
[88] Lundh O *et al* 2011 *Nat. Phys.* **7** 219
[89] Rechatin C *et al* 2009 Controlling the phase-space volume of injected electrons in a laser-plasma accelerator *Phys. Rev. Lett.* **102** 164801
[90] Brunetti E *et al* 2010 *Phys. Rev. Lett.* **105** 215007
[91] Fritzler S *et al* 2004 *Phys. Rev. Lett.* **92** 165006
[92] Leemans W P *et al* 2006 *Nat. Phys.* **2** 696
[93] Clayton C *et al* 2010 *Phys. Rev. Lett.* **105** 105003
[94] Lehe R *et al* 2013 *Phys. Rev. Lett.* **111** 085005
[95] Bucketal A *et al* 2013 *Phys. Rev. Lett.* **110** 185006
[96] Floettmann K 2003 *Phys. Rev. Spec. Top.—Accel. Beams* **6** 034202
[97] Antici P *et al* 2012 *J. Appl. Phys.* **112** 044902
[98] Migliorati M *et al* 2013 *Phys. Rev. Spec. Top.—Accel. Beams* **16** 011302
[99] Thaury C *et al* 2015 Demonstration of relativistic electron beam focusing by a laser-plasma lens *Nat. Commun.* **6** 6860
[100] Schlenvoigt H-P *et al* 2008 A compact synchrotron radiation source driven by a laser-plasma wakefield accelerator *Nat. Phys.* **4** 130–3
[101] Fuchs M *et al* 2009 Laser-driven soft-x-ray undulator source *Nat. Phys.* **5** 826
[102] Lambert G *et al* 2012 Progress on the generation of undulator radiation in the UV from a plasma- based electron beam *Proc. FEL Conf. (Nara, Japan)*
[103] Anania M P *et al* 2014 *Appl. Phys. Lett.* **104** 264102
[104] Nakajima K *et al* 1996 A table-top x-ray FEL based on the laser wakefield accelerator-undulator system *Nucl. Instrum. Methods* A **375** 593–6
[105] Schroder C B *et al* 2006 Design of an XUV FEL driven by the laser-plasma accelerator at the LBNL LOASIS facility *Proc. FEL06* (*Berlin, Germany*) pp 455–8
[106] Gruner F *et al* 2007 *Appl. Phys.* B **86** 431
[107] Anania M P *et al* 2010 The ALPHA-X beam line: towards a compact FEL *Proc. IPAC10 (Kyoto, Japan)* pp 2263–5
[108] Nakajima K 2008 Towards a table-top free-electron laser *Nat. Phys.* **4** 92
[109] Maier A R, Meseck A, Reiche S, Schroeder C B, Seggebrock T and Grüner F 2012 Demonstration scheme for a laser-plasma-driven free-electron laser *Phys. Rev. X* **2** 031019
[110] Seggebrock T, Maier A R, Dornmair I and Grüner F 2013 Bunch decompression for laser-plasma driven free-electron laser demonstration schemes *Phys. Rev. Spec. Top.—Accel. Beams* **16** 070703
[111] Couprie M E, Loulergue A, Labat M, Léhé R and Malka V 2014 Towards free electron laser with laser plasma accelerators *J. Phys. B: At. Mol. Opt. Phys.* **47** 234001 (12 pp) Special issues on compact x-ray sources
[112] Loulergue A, Labat M, Benabderrahmane C, Malka V and Couprie M E 2015 Beam manipulation for compact laser wakefield accelerator based free-electron lasers *New J. Phys.* **17** 023028
[113] Schroder C B *et al* 2012 *Proc. FEL 2012 (Nara, Japan)* pp 658–61
[114] Schroder C B *et al* 2013 *Proc. FEL2013 (New York, USA)* pp 117–21
[115] Maier A *et al* 2016 *Plasma Phys. Control. Fusion* in preparation
[116] Couprie M E *et al* 2014 *Proc. FEL'14 (Basel, Switzerland)* pp 574–9
[117] Labat M *et al* 2014 *Proc. FEL'14 (Basel, Switzerland)* pp 569–73
[118] Loulergue A *et al* 2015 *Proc. SPIE (Prague, April 2015)*
[119] Smith T *et al* 1979 *J. Appl. Phys.* **50** 4580
[120] Kroll N M *et al* 1981 Theory of the transverse gradient wiggler *IEEE J. Quantum Electron.* **17** 1496–507
[121] Huang Z *et al* 2012 Compact x-ray free-electron laser from a laser-plasma accelerator using a transverse-gradient undulator *Phys. Rev. Lett.* **109** 204801
[122] Baxevanis P *et al* 2014 3D theory of a high-gain free-electron laser based on a transverse gradient undulator *Phys. Rev. Spec. Top.—Accel. Beams* **17** 020701
[123] Baxevanis P *et al* 2015 Eigenmode analysis of a high-gain free-electron laser based on a transverse gradient undulator *Phys. Rev. Spec. Top.—Accel. Beams* **18** 010701
[124] Widmann C *et al* 2014 Beam transport system from a laser wakefield accelerator to a transverse gradient undulator *Proc. of IPAC2014 (Dresden, Germany)* pp 2803–6
[125] Widmann C *et al* 2015 First tests of a beam transport system from a laser wakefield accelerator to a transverse gradient undulator *Proc. of IPAC2015 (Richmond, USA)*
[126] Bernhard A *et al* 2015 Compact in-vacuum quadrupoles for a beam transport system at a laser wakefield accelerator *Proc. of IPAC2015 (Richmond, USA)*
[127] Fuchert G *et al* 2012 A novel undulator concept for electron beams with a large energy spread *Nucl. Instrum. Methods* A **672** 33–7

[128] Rodríguez V A *et al* 2013 Development of a superconducting transverse-gradient undulator for laser-wakefield accelerators *IEEE Trans. Appl. Supercond.* **23** 4101505
[129] Rodriguez V A *et al* 2015 Construction and first magnetic field test of a superconducting transversal gradient undulator for the laser wakefield accelerator in Jena *Proc. of IPAC2015 (Richmond, USA)*
[130] Berhnard A *et al* 2015 Transverse gradient undulator based high gain FELs- a parameter study *Proc. of IPAC2015 (Richmond, USA)*
[131] Reiche S 1999 A fully 3D time dependent FEL simulation code *Nucl. Instrum. Methods* A **429** 243–8
[132] Loulergue A *et al* 2015 COXINEL baseline reference case *LUNEX5/COXINEL Report* 2015
[133] Payet J private communications on Beta code
[134] Floettman K http://www.desy.de/~mpyflo/ page ASTRA code
[135] Kalmykov S Y *et al* 2012 *New J. Phys.* **14** 033025
[136] Chubar O, Elleaume P and Chavanne J 1998 A three-dimensional magnetostatics computer code for insertion devices *J. Synchrotron Radiat.* **5** 481–4
[137] TOSCA, OPERA-3d http://chilton-computing.org.uk/inf/eng/electromagnetics/p001.htm and http://operafea.com/
[138] Labat M *et al* 2014 Electron beam diagnostics for COXINEL *Proc. FEL'14 (Basel, Switzerland)*
[139] Keil B *et al* 2013 Design of the Swiss FEL BPM System *TUPC25, IBIC2013 (Oxford, UK)*
[140] Benabderrahmane C *et al* 2012 $Nd_2Fe_{14}B$ and $Pr_2Fe_{14}B$ magnets characterisation and modelling for cryogenic permanent magnet undulator applications *Nucl. Instrum. Methods Phys. Res.* A **669** 1–6
[141] Benabderrahmane C *et al* 2011 Development of $Pr_2Fe_{14}B$ cryogenic undulator CPMU at SOLEIL *Proc. Free Electron Laser (Shanghai, China)*
[142] Couprie M E *et al* 2015 Cryogenic undulators *Proc. SPIE (Prague, April 2015)*
[143] Valléau M *et al* 2015 Development of cryogenic undulators with PrFeB magnets at SOLEIL *Proc. SRI (New York, USA)*